JACS
JOURNAL OF THE AMERICAN CHEMICAL SOCIETY
Article
pubs.acs.org/JACS

# Photoelectrochemical Reduction of $CO_2$ Coupled to Water Oxidation Using a Photocathode with a Ru(II)−Re(I) Complex Photocatalyst and a $CoO_x$/TaON Photoanode

Go Sahara,[†] Hiromu Kumagai,[†] Kazuhiko Maeda,[†] Nicolas Kaeffer,[‡] Vincent Artero,[§] Masanobu Higashi,[§] Ryu Abe,[*,§] and Osamu Ishitani[*,†]

[†]Department of Chemistry, School of Science, Tokyo Institute of Technology, O-okayama 2-12-1-NE-1, Meguro-ku, Tokyo 152-8550, Japan

[‡]Laboratoire de Chimie et Biologie des Métaux, Université Grenoble Alpes, CNRS UMR 5249, CEA, F-38000 Grenoble, France

[§]Department of Energy and Hydrocarbon Chemistry, Graduate School of Engineering, Kyoto University, Katsura, Nishikyo-ku, Kyoto 615-8510, Japan

Supporting Information

**ABSTRACT:** Photoelectrochemical $CO_2$ reduction activity of a hybrid photocathode, based on a Ru(II)−Re(I) supramolecular metal complex photocatalyst immobilized on a NiO electrode (NiO−**RuRe**), was confirmed in an aqueous electrolyte solution. Under half-reaction conditions, the NiO−**RuRe** photocathode generated CO with high selectivity, and its turnover number for CO formation reached 32 based on the amount of immobilized **RuRe**. A photoelectrochemical cell comprising a NiO−**RuRe** photocathode and a $CoO_x$/TaON photoanode showed activity for visible-light-driven $CO_2$ reduction using water as a reductant to generate CO and $O_2$, with the assistance of an external electrical (0.3 V) and chemical (0.10 V) bias produced by a pH difference. This is the first example of a molecular and semiconductor photocatalyst hybrid-constructed photoelectrochemical cell for visible-light-driven $CO_2$ reduction using water as a reductant.

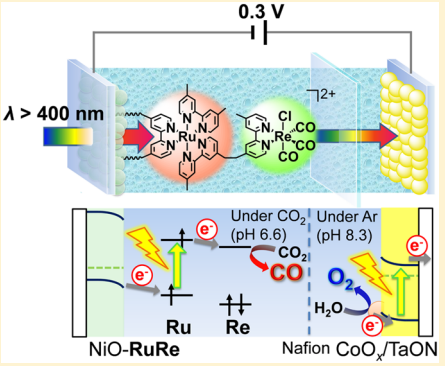


## INTRODUCTION

Photocatalytic $CO_2$ reduction to produce high-energy compounds using sunlight as an energy source, so-called artificial photosynthesis, is a promising means for constructing a sustainable and carbon-neutral society. Metal complex photocatalysts have been intensively investigated as key players in photochemical $CO_2$ reduction systems.[1−3] In particular, supramolecular metal complexes comprising both photosensitizer and catalyst units connected with bridging ligands have demonstrated high selectivity, durability, and quantum efficiency for $CO_2$ reduction under visible light irradiation.[4−14] These metal complex photocatalysts required a sacrificial reductant for driving the $CO_2$ reduction due to the low oxidizing ability of the photosensitizer unit, which is insufficient strength to utilize water as a reductant.

With the aim of visible-light-driven photocatalytic $CO_2$ reduction using water as a reductant, hybrid photocatalytic systems consisting of two kinds of photocatalysts, i.e., metal complexes and semiconductor materials, have been proposed.[15−18] In these systems, two photons are required for a Z-scheme-type stepwise excitation to produce both an electron with strong reducing power for $CO_2$ reduction and a hole with strong oxidizing power for a nonsacrificial electron donor such as methanol or water. Reported hybrid photocatalytic systems have been successfully constructed, and some have achieved $CO_2$ reduction with conversion of photon energy to chemical energy using methanol as an electron donor; however, the utilization of water as a reductant has not been reported.[15,19] Also, there are two other reports of hybrid systems comprising two or more semiconductor materials as light absorbers and metal complexes that exhibit relatively high activities to form formic acid and $O_2$ from $CO_2$ and water.[20−22] One was constructed with two semiconductor photoelectrodes and a cathodic side hybridized with a Ru(II) catalyst for $CO_2$ reduction. The other system used the combination of an amorphous silicon−germanium solar cell with the same Ru catalyst. The former system required the use of $TiO_2$ or $SrTiO_3$ as a photoanode necessitating UV light for excitation. The latter system used a triple-junction solar cell for producing both high-energy electrons and holes. In both cases, the use of extremely expensive materials, i.e., single-crystalline InP or the tandem solar cell, was required. In addition, the metal complexes were only used as catalysts for $CO_2$ reduction and not for photocatalysts in these hybrid systems. Thus, the hybrid photocatalytic system composed of both molecular and semiconductor photocatalysts for visible-light-driven $CO_2$ reduction using water as a reductant has not yet been realized.

**Received:** September 1, 2016
**Published:** October 2, 2016




DOI: 10.1021/jacs.6b09212
J. Am. Chem. Soc. 2016, 138, 14152−14158

Recently, we reported a novel hybrid photoelectrode consisting of a Ru(II)−Re(I) supramolecular metal complex photocatalyst (**RuRe**) and a NiO electrode for photoelectrochemical $CO_2$ reduction in a nonaqueous solution.[23] Visible light irradiation of the immobilized **RuRe** was shown to drive highly selective $CO_2$ reduction using electrons supplied from an external electric circuit through the p-type NiO semiconductor electrode, of which excitation was not necessary. If a cell, which used a counter photoanode composed of visible-light-driven semiconductor photocatalyst for water oxidation, e.g., TaON,[24,25] was constructed with the above-mentioned photocathode, $CO_2$ reduction could proceed under visible light irradiation using the electrons generated through water oxidation. Moreover, in such a tandem cell design, the photocatalyst for $CO_2$ reduction can be separated from the photoanode so as to suppress the back oxidation of products. Finally, the photocatalytic materials for $CO_2$ reduction and water oxidation can be individually designed and optimized in such a total tandem system. Therefore, developing these types of hybrid photoelectrochemical cells could be a first step in the realization of $CO_2$ reduction with simultaneous water oxidation using visible light as the energy source.

Herein, we report a novel hybrid photoelectrochemical cell for $CO_2$ reduction that uses water as the electron donor, composed of a NiO−**RuRe** hybrid photocathode and a $CoO_x$/TaON photoanode. First, we clearly demonstrate that the NiO−**RuRe** photocathode can drive the photocatalytic reduction of $CO_2$ in an aqueous electrolyte solution. Next, the photocathode was successfully combined with the $CoO_x$/TaON photoanode to drive water oxidation under visible light irradiation in a functional photoelectrochemical cell.

## EXPERIMENTAL SECTION

**Materials.** Acetonitrile was distilled three times over $P_2O_5$ and once over $CaH_2$ immediately before use. Pluronic F-88 was kindly supplied by BASF. $^{13}CO_2$ ($^{13}C$ = 99%) was purchased from CIL. $NaH^{13}CO_3$ ($^{13}C$ = 98%) was purchased from Aldrich. $H_2{}^{18}O$ ($^{18}O$ = 98%) was purchased from CMR and diluted with nonlabeled water to 30% as $H_2{}^{18}O$. Other reagents and solvents were commercial grade quality and used without further purification.

**General Procedure.** (Photo)electrochemical measurements were conducted using a potentiostat (ALS/CHI 620 or ALS/CHI 760e). A 300 W Xe lamp (Asahi Spectrum, MAX-302) with an IR-cut mirror module and a band-pass filter (Asahi Spectrum, MX0460 for irradiation of $\lambda$ = 460 nm) or cutoff filters (HOYA, L42 and Y48 for irradiation of $\lambda$ > 400 nm and $\lambda$ > 460 nm, respectively) was utilized for light irradiation. Product analysis of CO and $H_2$ in the gas phase was performed by means of gas chromatography (Inficon, MGC3000A). HCOOH in the liquid phase was checked using a capillary electrophoresis system (Otsuka Electronics, Capi-3300I). Evolved oxygen in the liquid phase was measured by Clark-type oxygen sensor (Unisense OX-N). GC−MS analysis of the gas phase of the reaction chamber was conducted using a gas chromatograph equipped with a mass spectrometer (Shimadzu, QP-2010-Ultra, Molsieve5A capillary column (30 m)). The X-ray photoelectron spectroscopy (XPS) measurement was conducted using ESCA-3400 (Shimadsu). The binding energy of the impurity carbon (1s) peak was adjusted to 284.6 eV to correct the chemical shifts of each element. Attenuated total reflection infrared spectroscopy (ATR-IR) was measured using FT/IR-4600 (JASCO).

**Preparation of the NiO−Metal Complex Hybrid Electrodes.** The NiO−metal complex hybrid electrode was prepared as reported previously.[23] Details of structural characterization of the electrode are shown in our previous paper.[23] Briefly, a precursor solution consisting of $Ni(NO_3)_2{\cdot}6H_2O$ (1.0 g, 99.95% KANTO chemicals) and Pluronic F-88 (0.5 g) dissolved in water/ethanol (4.5 g, 1:2, w/w) was deposited on cleaned FTO glass (AGC fabritech, 15 × 50 mm$^2$, 12 Ω/sq) by the doctor blade method with a glass rod using Scotch mending tape as a spacer. The obtained sample was calcined at 773 K for 30 min in air. This deposition−calcination cycle was repeated four times. The electrode was cut in half before use and immersed in a solution of acetonitrile with metal complex (4 mL, 10 $\mu$M) overnight. The electrode was washed with acetonitrile after hybridization. The adsorption amount of the metal complex was estimated by the difference in the absorbance of the metal to ligand charge transfer (MLCT) absorption band of the solution (at 461 nm) before and after hybridization.

**Preparation of the $CoO_x$/TaON Electrode.** The $CoO_x$/TaON electrode was prepared via a reported procedure.[25] Details of structural characterization of the electrode are shown in our previous paper.[25] TaON powder was prepared by heating $Ta_2O_5$ powder under $NH_3$ flow (20 mL min$^{-1}$) at 1123 K for 15 h. $CoO_x$ nanoparticles (5 wt % as metal) were loaded on TaON particles by impregnation from an aqueous $Co(NO_3)_2$ solution, followed by heating at 673 K for 30 min in air. As-prepared $CoO_x$-loaded TaON particles were deposited on a Ti substrate by electrophoretic deposition. The electrodes were treated with 50 $\mu$L of $TaCl_5$ methanol solution (10 mM) and then dried in air at room temperature. After this process was performed five times, the electrode was heated in $NH_3$ flow (10 mL min$^{-1}$) at 723 K for 30 min.

**Estimation of Electrochemically Active RuRe Species on NiO−RuRe.** The estimations of the electrochemically active **RuRe** species on the photoelectrode were conducted by cyclic voltammetry using a three-electrode setup. An Ar-purged $CH_3CN$ containing 0.1 M $Et_4NBF_4$ was used as electrolyte. A Pt wire and a Ag wire in 0.01 M $AgNO_3$ acetonitrile solution were employed as the counter and reference electrodes, respectively. The scan rate was set to 50 mV s$^{-1}$, and the amount of electrochemically active Ru unit was calculated using eq 1 from the second cycles of each sample.

$$n = S/Fv \tag{1}$$

Here, $n$ is the amount of electrochemically active Ru unit (mol), and $S$ is the area of the oxidation peak of Ru(II/III) (A V). $F$ is the Faraday constant (96 485 C mol$^{-1}$), and $v$ is the sweep rate (V s$^{-1}$).

**Photoelectrochemical $CO_2$ Reduction Using NiO−RuRe.** Photoelectrochemical $CO_2$ reduction was conducted using an O-ring-sealed Pyrex cell and a stirring tip. The total volume of the cell without the stirring tip and electrodes was ca. 130 mL, and 84 mL of a $CO_2$-saturated 50 mM $NaHCO_3$ (KANTO chemical) aqueous solution (pH 6.6) was used as the electrolyte; therefore, the estimated gas phase was ca. 46 mL. The reaction was conducted after purging with $CO_2$ for more than 40 min. A three-electrode setup was used through the photoelectrochemical measurement and $CO_2$ reduction reaction. A Pt wire and Ag/AgCl in saturated KCl aqueous solution were employed as the counter and reference electrodes, respectively. The counter electrode was separated from the reaction solution by Vycor glass to prevent the influence of oxidization reaction taking place on the counter electrode, of which the oxidation product(s) was not measured. The geometric area of working electrode was ca. 2.5 cm$^2$.

**Photoelectrochemical Water Oxidation Using $CoO_x$/TaON.** Photoelectrochemical water oxidation was conducted using an O-ring-sealed Pyrex cell with a total volume of ca. 16 mL. A 10 mL portion of an Ar-purged 50 mM $NaHCO_3$ aqueous solution (pH 8.3) was used as the electrolyte. The reaction was conducted after purging with Ar for more than 30 min. A three-electrode setup was used through the photoelectrochemical measurement and water oxidation reaction. A Pt wire and Ag/AgCl in saturated KCl aqueous solution were employed as the counter and reference electrodes, respectively. The counter electrode was separated from the reaction solution by Nafion membrane (Aldrich, Nafion 117). The active geometric area of working electrode was ca. 1.1 cm$^2$.

**Photoelectrochemical $CO_2$ Reduction Using Hybrid Electrochemical Cell with Z-Scheme Configuration.** The reaction was conducted using the electrochemical cell with two chambers (ca. 16 mL for each chamber) divided by Nafion membrane (Aldrich, Nafion 117), and the photoelectrodes were installed into each chamber


DOI: 10.1021/jacs.6b09212
J. Am. Chem. Soc. 2016, 138, 14152−14158

individually. The active geometric area of each electrode was ca. 1.1 $cm^2$. A 10 mL portion of a 50 mM $NaHCO_3$ aqueous solution was added as an electrolyte to both chambers and purged with $CO_2$ for the cathode chamber (pH = 6.6) and with Ar for the anode chamber (pH = 8.3), respectively. Light irradiation was conducted from the back side of the NiO−**RuRe** photocathode, and the light which transmitted through the NiO−**RuRe** and the Nafion membrane was irradiated to the $CoO_x$/TaON photoanode (Figure 6). An electrical bias of −0.3 V vs $CoO_x$/TaON was applied for NiO−**RuRe** using a potentiostat to accelerate the reaction. We note that prereaction using $CoO_x$/TaON was conducted under 400 nm light with an applied potential of +0.5 V versus Ag/AgCl up to 10 mC as the electric charge which passed through the circuit in order to remove the organic substance on the electrode surface and to improve the Faraday efficiency for water oxidation. An isotope tracer experiment was conducted using water containing 30% $H_2{}^{18}O$ and $NaHCO_3$ (50 mM) as a solvent for the anode chamber. After bubbling with He instead of $^{36}Ar$ which has the same molecular weight as $^{18}O_2$ into the anode chamber and with $CO_2$ into the cathode chamber for 30 min, visible light was irradiated for 60 min with the bias of −0.3 V by using the same system as described above. The products in the gas phase of the anode chamber were analyzed by GC−MS by sampling using a syringe through a septum after the irradiation.

## RESULTS AND DISCUSSION

In the hybrid photocathode, NiO−**RuRe**, **RuRe** with two methylphosphonic acid groups as anchors (Chart 1) was immobilized on the surface of a p-type semiconductor NiO electrode consisting of fluorine doped tin oxide (FTO) glass coated with a NiO film (active area: ca. 2.5 $cm^2$).[23] Photoelectrochemical measurements using the NiO−**RuRe** photocathode were conducted to examine its activity for reducing $CO_2$ in an aqueous solution. Figure 1 shows the current−potential curve of the NiO−**RuRe** photocathode under irradiation at $\lambda$ = 460 nm, at which the photoexcitation of NiO cannot occur, in a $CO_2$-purged aqueous solution containing 50 mM $NaHCO_3$ (pH = 6.6); a photocathodic response was clearly observed starting at approximately −0.1 V vs Ag/AgCl. This behavior was similar to that observed in an organic solution, i.e., a 5:1 v/v *N*,*N*-dimethylformamide and triethanolamine mixture containing $Et_4NBF_4$ (0.1 M) as an electrolyte,[23] and the photoresponse can be attributed to electron transfer from the valence band of the NiO electrode to the excited Ru photosensitizer unit in **RuRe**. These results strongly suggest that photoelectrochemical $CO_2$ reduction proceeded using the NiO−**RuRe** photocathode in the aqueous solution.

**Chart 1. Structures of Metal Complexes**

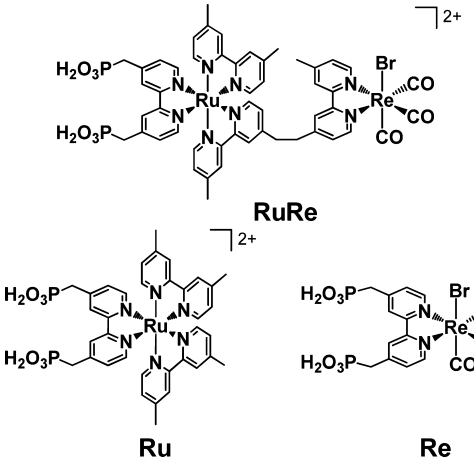


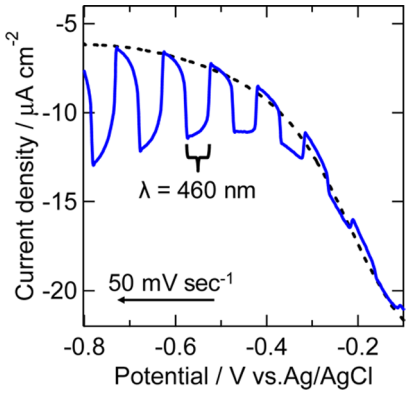


**Figure 1.** Current−potential curve of NiO−**RuRe** with intermittent irradiation ($\lambda$ = 460 nm) in a $CO_2$-purged 50 mM $NaHCO_3$ aqueous solution (pH = 6.6). Dotted line indicates the *I*−*E* curve under dark conditions.

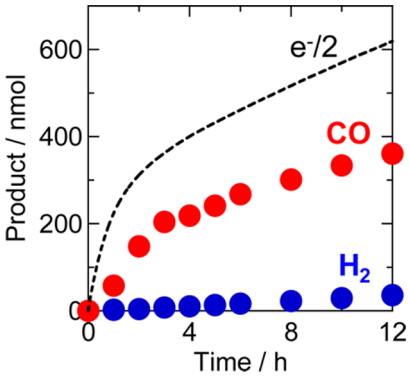


**Figure 2.** Time course of gaseous products during irradiation of NiO−**RuRe** photocathode at −0.7 V vs Ag/AgCl under a $CO_2$ atmosphere ($\lambda$ > 460 nm).

As a typical run for the photoelectrochemical reactions, the NiO−**RuRe** photocathode with an applied bias of −0.7 V vs Ag/AgCl in an aqueous solution was irradiated at $\lambda$ > 460 nm using a 300 W Xe lamp with a cutoff filter. Figure 2 shows the time course of the generated products that consist mainly of CO with a very small amount of $H_2$ and half of the electrons which passed through the outer circuit of the photoelectrochemical cell; 361 nmol of CO was produced with 12 h irradiation yielding a turnover number ($TON_{CO}$) of 32 based on the amount of **RuRe** adsorbed on the NiO electrode. The selectivity of CO ($SL_{CO}$) was very high, especially in the first stage ($SL_{CO}$ > 95%). After an induction period, the formation of $H_2$ increased, but total $SL_{CO}$ was still 91% for 12 h of irradiation. Other gaseous products were not detected. The electrons which could not be assigned for the CO formation might be consumed for reduction of the trivalent nickel ions ($Ni^{3+}$) in NiO at the initial stage of the reaction, which was observed in similar photoelectrochemical reactions in both organic and aqueous solutions,[23,26] and another possibility is formation of a small amount of formic acid via $CO_2$ reduction which should be lower than the detection limit of formate with the capillary electrophoresis analyzer (about 2 $\mu$mol in the solution). Formation of CO did not proceed without irradiation or under an Ar-only atmosphere (entry 7 in Table 1).



DOI: 10.1021/jacs.6b09212
J. Am. Chem. Soc. 2016, 138, 14152−14158

**Table 1. Photoelectrochemical $CO_2$ Reduction Using Various Electrodes**[a]

| entry | sample | complex/nmol | potential/V[b] | CO/nmol ($TON_{CO}$) | $H_2$/nmol | $F_{red}$/% |
|---|---|---|---|---|---|---|
| 1 | NiO−**RuRe** | 11.2 | −0.7 | 241 (22) | 13 | 59 |
| | | | | 361 (32)[c] | 36[c] | 64[c] |
| 2 | NiO−**RuRe** | 10.3 | −0.3 | 111 (11) | 10 | 45 |
| 3 | NiO−**RuRe** | 9.6 | 0 | n.d. | n.d. | |
| 4 | NiO−**Ru** | 11.5 | −0.7 | n.d. | 21 | 21 |
| 5 | NiO−**Re** | 15.9 | −0.7 | n.d. | n.d. | |
| 6[d] | NiO−**RuRe** | 10.2 | −0.7 | n.d. | n.d. | |
| 7[e] | NiO−**RuRe** | 9.4 | −0.7 | n.d. | 11 | 56 |

[a]Electrode was irradiated at $\lambda > 460$ nm for 5 h in 50 mM $NaHCO_3$ aq solution under a $CO_2$ atmosphere. [b]Versus Ag/AgCl (sat. KCl). [c]12 h irradiation. [d]In the dark. [e]Under an Ar atmosphere.

For clarification of the carbon source(s) of the produced CO, a similar photoelectrochemical reaction was conducted with $NaH^{13}CO_3$ as an electrolyte under a $^{13}CO_2$ atmosphere (C-13 labeled gas and electrolyte were used to prevent equilibrium redistribution of the labeled isotope). GC−MS analysis revealed that $^{13}CO$ was produced, and $^{12}CO$ was not clearly detected (Figure 3). Therefore, the carbon source of CO was confirmed to be $CO_2$ either as introduced or formed from the $NaHCO_3$ electrolyte.

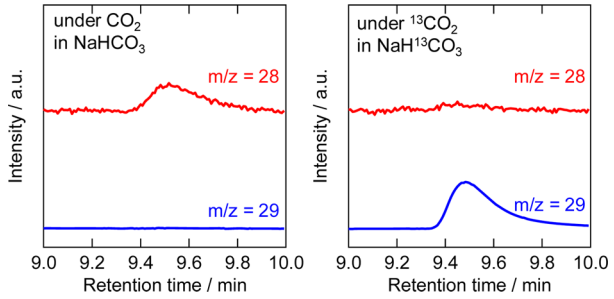


**Figure 3.** GC−MS chart of evolved CO in the gas phase during photoelectrochemical $CO_2$ reduction using NiO−**RuRe** in an aqueous solution containing 50 mM $NaHCO_3$ under $CO_2$ (left) or 50 mM $NaH^{13}CO_3$ under $^{13}CO_2$ (right).

Table 1 summarizes the results of the photoelectrochemical reactions conducted under different applied biases; the corresponding $I-t$ curves are shown in Figure S1. The photocurrent and CO evolution are relatively small at −0.3 V (entry 2) compared to those at −0.7 V (entry 1), and become almost zero at 0 V (entry 3). Correlation between photocurrent and CO evolution clearly suggests a mechanism in which electrons are supplied to the immobilized **RuRe** through the NiO electrode for the reduction of $CO_2$. Formation of CO did not proceed in the cases using the model mononuclear complexes of either the photosensitizer Ru(II) unit (**Ru** in Chart 1) or the Re(I) catalyst unit (**Re**) instead of the **RuRe** (entries 4 and 5) complex. An induction period for the generation of $H_2$ using NiO−**RuRe** was observed for the first 2 h (Figure S2), and the $H_2$ formation was also observed even using NiO−**Ru** instead of NiO−**RuRe** (entry 4 in Table 1, $TON_{H2} = 2$). These results strongly suggest that the $H_2$ was derived from photocatalysis of the degraded product of the Ru photosensitizer, such as $[Ru^{II}(N^{\wedge}N)_2(L)_2]^{n+}$ (L = solvent), during the irradiation. Such a phenomenon has been reported in homogeneous photocatalytic systems using a Ru(II)−Re(I) binuclear complex in an aqueous solution.[14,27]

The results described above demonstrated that the NiO−**RuRe** hybrid photocathode is capable of driving photoelectrochemical $CO_2$ reduction with high selectivity under visible light in an aqueous solution; however, the $TON_{CO}$ of the NiO−**RuRe** photocathode (32) was lower than the reported value of 130 for the homogeneous system that used a sacrificial electron donor in an aqueous solution.[14] In order to investigate the source of this difference, the electrochemically active amount of **RuRe** on the NiO−**RuRe** electrode was estimated using cyclic voltammetry in an acetonitrile solution (Figure 4, left, and entry 1 in Table 2). In the first scan, a reversible redox system and an irreversible oxidation wave were observed,

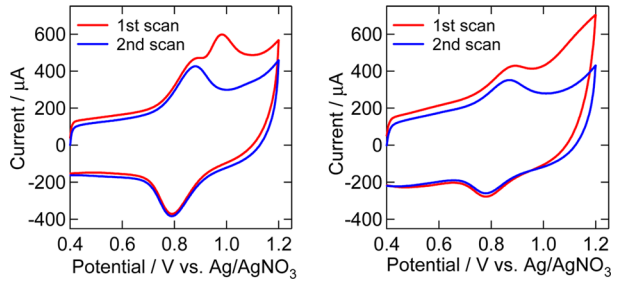


**Figure 4.** Cyclic voltammograms of NiO−**RuRe** (left) and after reaction (right) in an Ar-purged $CH_3CN$ containing 0.1 M $Et_4NBF_4$ as electrolyte. Scan rate was 50 mV $s^{-1}$.

attributable to the Ru(II/III) of the Ru unit and Re(I/II) of the Re unit, respectively. The second scan using the same electrode showed only a reversible wave, consistent with previous reports that indicate oxidation of a $[Re^{I}(diimine)(CO)_3X]^{+}$-type complex to induce decomposition of the complex.[28] Therefore, only the Ru unit should be electrochemically active during the second scan. Additional scans did not affect the shape or area of the reversible redox peak. Owing to the simplicity of the CV wave, we chose the second wave for estimating the amount of the electrochemically active **RuRe**, which should be almost the same as the remaining Ru unit in the second scan. The amount of electrochemically active **RuRe** on the NiO electrode was estimated to be 6.5 nmol, lower than the total adsorbed amount of **RuRe** on the NiO electrode before the photocatalytic reaction (9.7 nmol), indicating that only two-thirds of **RuRe** in NiO−**RuRe** was present to accept electrons from the NiO electrode; in other words, only two-thirds of the starting complex is active for the photocatalytic $CO_2$ reduction. Cyclic voltammetry using the electrode after the photoelectrochemical reaction for 5 h was also conducted using the same procedure (Figure 4, right, and entry 2 in Table 2).[29] The amount of electrochemically active **RuRe** was reduced to 2.9 nmol. These


DOI: 10.1021/jacs.6b09212
J. Am. Chem. Soc. 2016, 138, 14152−14158

**Table 2. Estimated Amounts of RuRe on the NiO−RuRe Electrodes**

| entry | estimated amount of **RuRe**/nmol | | (CV)/(absorbance) |
|---|---|---|---|
| | adsorbed (from absorbance) | electrochemically active (from CV) | |
| 1 (as-prepared) | 9.7 | 6.5 | 0.67 |
| 2 (after reaction) | 9.2 | 2.9 | 0.32 |

results suggest that one-third of the total amount of **RuRe** immobilized on the NiO electrode is natively inactive, even before irradiation, likely due to low conductivity in some areas of the NiO electrode, and half of the active **RuRe** is lost to photocatalysis during irradiation for 5 h. XPS measurements were also conducted to reveal the electronic state and abundance ratio of elements on the NiO−**RuRe** surface before and after the photoelectrochemical reaction (Figure S3). No obvious change of the electronic state was observed. Unfortunately, the peak of the Ru 3d partially overlapped with that of the carbon 1s (285 eV), making assignment difficult, but the Re/Ni ratio decreased from 0.028 to 0.013 after the photoelectrochemical reaction. The decrease of the Re complex on the electrode was consistent with that of the Ru complex obtained by using the cyclic voltammetry as discussed above. ATR-IR measurement confirmed that the tricarbonyl structure of the Re unit on the electrode was maintained after the photoelectrochemical reaction; however, the strength of the band became weaker (Figure S4). Therefore, desorption of **RuRe** from the NiO surface and photochemical decomposition of **RuRe** are likely sources for the relatively low $TON_{CO}$. Desorption of metal complexes with phosphonic acid anchor groups from the metal oxide surfaces has been reported, and was shown to be accelerated by irradiation.[30,31] Hence, suppression of photodesorption of the metal complex from the electrode should be a way to improve both the activity and stability of the hybrid photocathode.

In order to construct a full cell with the NiO−**RuRe** photocathode, photoelectrochemical water oxidation using a $CoO_x$/TaON photoanode, which has been reported as an efficient photoanode for the water splitting reaction,[25] was examined in an aqueous solution containing sodium bicarbonate (50 mM, pH = 8.3). The $CoO_x$/TaON electrode was prepared as previously reported.[25]

Figure 5 shows the current−potential curve of the $CoO_x$/TaON photoanode in a $NaHCO_3$ aqueous solution under an Ar atmosphere. The anodic photocurrent, which corresponds to water oxidation, was observed at a potential more positive

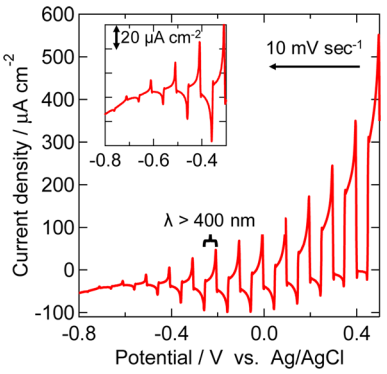


**Figure 5.** Current−potential curve of $CoO_x$/TaON photoanode with intermittent irradiation ($\lambda$ > 400 nm) in an Ar-purged 50 mM $NaHCO_3$ aqueous solution (pH = 8.3).

than −0.7 V vs Ag/AgCl, which is almost equivalent to the reported value measured in a $Na_2SO_4$ aqueous solution (pH 8).[25] Under these reaction conditions, formation of $O_2$ was observed in the liquid phase, which was detected using an $O_2$ sensor, and its total Faraday efficiency was 89% after 5 min of irradiation (Figure S5). Of note, we limited the time of the photoelectrochemical reaction to 5 min to avoid contamination from air. During this period, most of the evolved $O_2$ remained in the liquid phase. On the basis of these data, we concluded that the $CoO_x$/TaON photoanode is active for water oxidation even in a $NaHCO_3$ aqueous solution.

Figure 6 shows a schematic representation of the hybrid photoelectrochemical cell consisting of the NiO−**RuRe** photo-

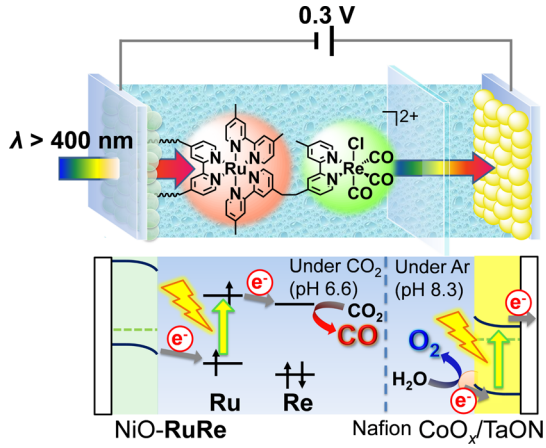


**Figure 6.** Schematic image of hybrid photoelectrochemical cell with Z-scheme configuration.

cathode and the $CoO_x$/TaON photoanode, with a Z-scheme configuration for $CO_2$ reduction using water as a reductant. In the photoelectrochemical cell, the photoanode was separated from the photocathode using a Nafion membrane. During the reaction, both CO and $H_2$ in the gas phase of the photocathode chamber were detected using micro-gas-chromatography. The evolved $O_2$ in the liquid phase of the photoanode chamber was detected using the $O_2$ sensor; however, the exact $O_2$ concentration in the gas phase could not be determined because of small amounts of contamination of air from outside the chamber. Visible light irradiation ($\lambda$ > 400 nm) was conducted from the backside of the NiO−**RuRe** photocathode; transmitted light penetrated through the NiO−**RuRe** and the Nafion membrane to be irradiated to the $CoO_x$/TaON photoanode. A bias of −0.3 V vs $CoO_x$/TaON was applied to NiO−**RuRe** using a potentiostat to accelerate the reaction. We note that there was also a chemical bias of 0.10 V from the pH difference between two electrodes.

Figure 7 shows the time course of the photocurrent and observed amounts of $O_2$ in the reaction solution in the chamber of the $CoO_x$/TaON photoanode with intermittent irradiation. Evolution of $O_2$ was observed only when the photoelectrochemical cell was irradiated, reaching 77 nmol with


DOI: 10.1021/jacs.6b09212
J. Am. Chem. Soc. 2016, 138, 14152−14158

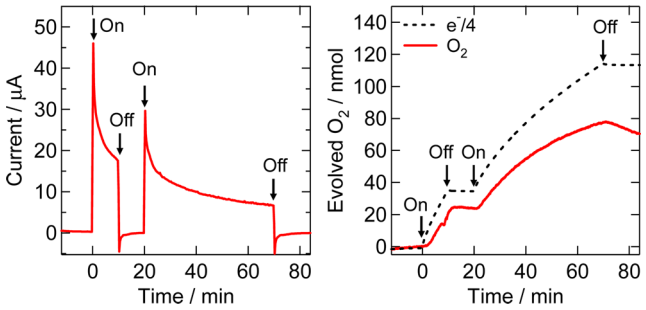


**Figure 7.** Time course of photocurrent of hybrid photoelectrochemical cell comprising NiO−**RuRe** and $CoO_x$/TaON under visible light irradiation ($\lambda$ > 400 nm) (left) and the amount of evolved oxygen in liquid phase (right). A combined electrical (0.3 V) and chemical (0.10 V) bias was applied.

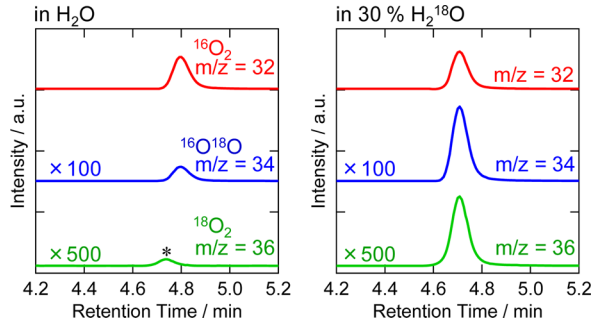


**Figure 8.** GC−MS chart of $O_2$ in gas phase of anode chamber during photoelectrochemical $CO_2$ reduction using Z-scheme configuration in $H_2O$ (left) or 30% $H_2{}^{18}O$ (right). * indicates $^{36}Ar$ derived from contamination of air through sampling.

68% Faradaic efficiency after 60 min of irradiation. Note that the $O_2$ detected in the liquid phase decreased after irradiation stopped, as shown in Figure 7. This indicates that diffusion of the $O_2$ from the liquid phase to the gas phase proceeds, but the rate was slow, even after 60 min of irradiation (38 nmol $h^{-1}$). The produced CO was simultaneously detected in the gas phase in the NiO−**RuRe** photocathode chamber; 79 nmol of CO was evolved for 60 min of irradiation, corresponding to a $TON_{CO}$ = 17 based on the amount of immobilized **RuRe** before irradiation. Total Faradaic efficiency of the cathodic reaction, including $H_2$ evolution (6 nmol), was 37%. The difference of the Faradaic efficiencies between the anodic and cathodic reactions could be mainly caused by the reduction of trivalent nickel ions ($Ni^{3+}$) that originally existed in NiO on the photocathode, as observed in similar photoelectrochemical reactions in both organic and aqueous solutions.[23,26] The photoelectrochemical cell without the **RuRe** photocatalyst did not produce any reduction products of $CO_2$ in the photocathode chamber, and the increase of $O_2$ in the photoanode chamber was very small (<20 nmol) for 60 min irradiation under the same reaction condition.

An isotope tracer experiment using water containing 30% $H_2{}^{18}O$ and $NaHCO_3$ (50 mM) as the solvent was conducted. This solution was added to the anode chamber of the cell, and after He was bubbled into the anode chamber and $CO_2$ into the cathode chamber for 30 min, both electrodes were irradiated with visible light for 60 min with a bias of −0.3 V using the same system described above (Figure 6). The products in the gas phase of the anode chamber were analyzed by GC−MS. The results are summarized in Figure 8. The ratios of $^{16}O^{18}O$ and $^{18}O_2$ were significantly larger when using 30% $H_2{}^{18}O$ ($^{16}O^{18}O$, 1.9%; $^{18}O_2$, 0.38%) than those for the reaction using nonlabeled water ($^{16}O^{18}O$, 0.44%; $^{18}O_2$, <0.01%); however, they were different than the theoretically expected ratios if all the $O_2$ was produced from water ($^{16}O^{18}O$, 42%; $^{18}O_2$, 9%) without any exchange of the oxygen atoms with other substrates during the photoelectrochemical reaction. Involvement of O atoms from the $CoO_x$ oxygen evolution catalyst is a possible explanation for such a result.[32] Exchange of $NaHC^{16}O_3$ by $^{18}O$ from $H_2{}^{18}O$ should also proceed during the photoelectrochemical reaction, and contamination from air when the syringe was used for sampling the gas phase in the anode chamber through the septum cannot be excluded. In the photoelectrochemical experiment (Figure 7), on the other hand, an oxygen sensor in the liquid phase was used for determining the produced amount of $O_2$ in solution to prevent overestimation of $O_2$. These results suggest that $O_2$ was, at least partially, generated by a water oxidation reaction driven by visible light irradiation.

Therefore, this photoelectrochemical cell is confirmed to drive $CO_2$ reduction to obtain CO and $O_2$ with visible light irradiation (eq 2).

$$CO_2 \rightarrow CO + 1/2O_2 \quad (2)$$

Despite the use of external electrical and chemical biases, this is the first instance of successful visible-light-driven $CO_2$ reduction using water as a reductant, accomplished by use of a molecular photocatalyst hybridized with a semiconductor photocatalyst. The light energy conversion efficiency of the reaction was calculated to be $1.6 \times 10^{-5}$, considering the electrical bias of 0.3 V and chemical bias of 0.10 V from the pH difference between the two electrolytes. The details of the calculation are described in the Supporting Information. The low performance of the photoelectrochemical system mainly arises from the photocathode. The NiO electrode substrate itself is problematic because of its low conductivity, and the presence of electrochemically inactive surface areas. In addition, desorption and photochemical degradation of **RuRe** from the NiO surface is the main reason for limited durability. Research studies to address such problems are now under way in our laboratory.

## CONCLUSION

We successfully developed a NiO−**RuRe** hybrid photocathode for photoelectrochemical $CO_2$ reduction in an aqueous solution and constructed a hybrid photoelectrochemical cell with a $CoO_x$/TaON photoanode that can drive water oxidation. Using visible light, the NiO−**RuRe** photocathode catalytically generated CO with high selectivity in aqueous solution. The hybrid photoelectrochemical cell consisting of the NiO−**RuRe** hybrid photocathode and the $CoO_x$/TaON photoanode showed activity for visible-light-driven catalytic reduction of $CO_2$ and oxidation of water to generate CO and $O_2$. To the best of our knowledge, this is the first example of a visible-light-driven $CO_2$ reduction system using water as the reductant, based on molecular photocatalysts hybridized with semiconductor photocatalysts.

## ASSOCIATED CONTENT

### Supporting Information

The Supporting Information is available free of charge on the ACS Publications website at DOI: 10.1021/jacs.6b09212.



DOI: 10.1021/jacs.6b09212
J. Am. Chem. Soc. 2016, 138, 14152−14158

Time courses of photocurrent of NiO−**RuRe** at various applied potential, time course of evolved $H_2$ during photoelectrochemical $CO_2$ reduction using NiO−**RuRe**, XPS spectra, ATR-IR spectra, time courses of photocurrent and amount of evolved oxygen using $CoO_x$/TaON, spectrum of irradiated light, and calculation method of light−energy conversion efficiency for hybrid photoelectrochemical cell (PDF)

## AUTHOR INFORMATION


### Corresponding Authors

*ryu-abe@scl.kyoto-u.ac.jp

*ishitani@chem.titech.ac.jp


### Notes

The authors declare no competing financial interest.

## ACKNOWLEDGMENTS

This work was supported by Strategic International Collaborative Research Program (PhotoCAT project) from both Japan Science and Technology Agency (JST) and the French National Research Agency (ANR-14-JTIC-0004-01) and CREST (Molecular Technology project, JST). This is also partially supported by a Grant-in-Aid for Scientific Research on Innovative Area "Artificial Photosynthesis" (Project 24107005) from the Japan Society for the Promotion of Science (JSPS) and the Photon and Quantum Basic Research Coordinated Development Program (MEXT, Japan). N.K. and V.A. acknowledge Labex program, ARCANE, ANR-11-LABX-0003-01 (French National Research Agency). K.M. acknowledges the Noguchi Institute, and the Murata Science Foundation.

## REFERENCES


(1) Morris, A. J.; Meyer, G. J.; Fujita, E. *Acc. Chem. Res.* **2009**, *42*, 1983−1994.

(2) Sahara, G.; Ishitani, O. *Inorg. Chem.* **2015**, *54*, 5096−5104.

(3) Yamazaki, Y.; Takeda, H.; Ishitani, O. *J. Photochem. Photobiol., C* **2015**, *25*, 106−137.

(4) Gholamkhass, B.; Mametsuka, H.; Koike, K.; Tanabe, T.; Furue, M.; Ishitani, O. *Inorg. Chem.* **2005**, *44*, 2326−2336.

(5) Sato, S.; Koike, K.; Inoue, H.; Ishitani, O. *Photochem. Photobiol. Sci.* **2007**, *6*, 454−461.

(6) Koike, K.; Naito, S.; Sato, S.; Tamaki, Y.; Ishitani, O. *J. Photochem. Photobiol., A* **2009**, *207*, 109−114.

(7) Tamaki, Y.; Morimoto, T.; Koike, K.; Ishitani, O. *Proc. Natl. Acad. Sci. U. S. A.* **2012**, *109*, 15673−15678.

(8) Tamaki, Y.; Watanabe, K.; Koike, K.; Inoue, H.; Morimoto, T.; Ishitani, O. *Faraday Discuss.* **2012**, *155*, 115−127.

(9) Tamaki, Y.; Koike, K.; Morimoto, T.; Ishitani, O. *J. Catal.* **2013**, *304*, 22−28.

(10) Tamaki, Y.; Koike, K.; Morimoto, T.; Yamazaki, Y.; Ishitani, O. *Inorg. Chem.* **2013**, *52*, 11902−11909.

(11) Kato, E.; Takeda, H.; Koike, K.; Ohkubo, K.; Ishitani, O. *Chem. Sci.* **2015**, *6*, 3003−3012.

(12) Tamaki, Y.; Koike, K.; Ishitani, O. *Chem. Sci.* **2015**, *6*, 7213−7221.

(13) Nakada, A.; Koike, K.; Nakashima, T.; Morimoto, T.; Ishitani, O. *Inorg. Chem.* **2015**, *54*, 1800−1807.

(14) Nakada, A.; Koike, K.; Maeda, K.; Ishitani, O. *Green Chem.* **2016**, *18*, 139−143.

(15) Sekizawa, K.; Maeda, K.; Domen, K.; Koike, K.; Ishitani, O. *J. Am. Chem. Soc.* **2013**, *135*, 4596−4599.

(16) Yoshitomi, F.; Sekizawa, K.; Maeda, K.; Ishitani, O. *ACS Appl. Mater. Interfaces* **2015**, *7*, 13092−13097.

(17) Kuriki, R.; Matsunaga, H.; Nakashima, T.; Wada, K.; Yamakata, A.; Ishitani, O.; Maeda, K. *J. Am. Chem. Soc.* **2016**, *138*, 5159−5170.

(18) Muraoka, K.; Kumagai, H.; Eguchi, M.; Ishitani, O.; Maeda, K. *Chem. Commun.* **2016**, *52*, 7886−7889.

(19) Nakada, A.; Nakashima, T.; Sekizawa, K.; Maeda, K.; Ishitani, O. *Chem. Sci.* **2016**, *7*, 4364−4371.

(20) Sato, S.; Arai, T.; Morikawa, T.; Uemura, K.; Suzuki, T. M.; Tanaka, H.; Kajino, T. *J. Am. Chem. Soc.* **2011**, *133*, 15240−15243.

(21) Arai, T.; Sato, S.; Kajino, T.; Morikawa, T. *Energy Environ. Sci.* **2013**, *6*, 1274.

(22) Arai, T.; Sato, S.; Morikawa, T. *Energy Environ. Sci.* **2015**, *8*, 1998−2002.

(23) Sahara, G.; Abe, R.; Higashi, M.; Morikawa, T.; Maeda, K.; Ueda, Y.; Ishitani, O. *Chem. Commun.* **2015**, *51*, 10722−10725.

(24) Abe, R.; Higashi, M.; Domen, K. *J. Am. Chem. Soc.* **2010**, *132*, 11828−11829.

(25) Higashi, M.; Domen, K.; Abe, R. *J. Am. Chem. Soc.* **2012**, *134*, 6968−6971.

(26) Kaeffer, N.; Massin, J.; Lebrun, C.; Renault, O.; Chavarot-Kerlidou, M.; Artero, V. *J. Am. Chem. Soc.* **2016**, *138*, 12308−12311.

(27) Kuramochi, Y.; Ishitani, O. *Inorg. Chem.* **2016**, *55*, 5702−5709.

(28) Bullock, J. P.; Carter, E.; Johnson, R.; Kennedy, A. T.; Key, S. E.; Kraft, B. J.; Saxon, D.; Underwood, P. *Inorg. Chem.* **2008**, *47*, 7880−7887.

(29) We note that there is no oxidation peak corresponding to the Re unit for the NiO−**RuRe** after the photoelectrochemical reaction, while that for the as-prepared unit was clearly observed in Figure 4 (left). The results suggest that a large positive shift of the oxidation potential of the Re unit was derived from ligand substitution. It could be generally considered that the Re catalyst ($Re(N^N)(CO)_3Br$) forms coordinately unsaturated intermediates by dissociation of the Br ligand during the reaction and could terminally change to solvent complexes ($[Re(N^N)(CO)_3L]^{n+}$). The positive shift in the oxidation potential in Figure 4 (right) was possibly caused by formation of an acetonitrile complex ($[Re(N^N)(CO)_3MeCN]^+$), which has lower energy for the $t_{2g}$ orbital compared to the original complex, through cyclic voltammetry in an acetonitrile solution.

(30) Hanson, K.; Brennaman, M. K.; Luo, H.; Glasson, C. R. K.; Concepcion, J. J.; Song, W.; Meyer, T. J. *ACS Appl. Mater. Interfaces* **2012**, *4*, 1462−1469.

(31) Hanson, K.; Brennaman, M. K.; Ito, A.; Luo, H.; Song, W.; Parker, K. A.; Ghosh, R.; Norris, M. R.; Glasson, C. R. K.; Concepcion, J. J.; Lopez, R.; Meyer, T. J. *J. Phys. Chem. C* **2012**, *116*, 14837−14847.

(32) Koroidov, S.; Anderlund, M. F.; Styring, S.; Thapper, A.; Messinger, J. *Energy Environ. Sci.* **2015**, *8*, 2492−2503.




DOI: 10.1021/jacs.6b09212
J. Am. Chem. Soc. 2016, 138, 14152−14158